ELSEVIER

Mathematical Biosciences 157 (1999) 217–236

Mathematical Biosciences
an international journal

# Resistance of a food chain to invasion by a top predator

B.W. Kooi *, M.P. Boer, S.A.L.M. Kooijman

*Faculty of Biology, Free University, De Boelelaan 1087, 1081 HV Amsterdam, The Netherlands*

Received 31 December 1997; received in revised form 19 August 1998; accepted 9 October 1998

**Abstract**

We study the invasion of a top predator into a food chain in a chemostat. For each trophic level, a bioenergetic model is used in which maintenance and energy reserves are taken into account. Bifurcation analysis is performed on the set of nonlinear ordinary differential equations which describe the dynamic behaviour of the food chain. In this paper, we analyse how the ability of a top predator to invade the food chain depends on the values of two control parameters: the dilution rate and the concentration of the substrate in the input. We investigate invasion by studying the long-term behaviour after introduction of a small amount of top predator. To that end we look at the stability of the boundary attractors; equilibria, limit cycles as well as chaotic attractors using bifurcation analysis. It will be shown that the invasibility criterion is the positiveness of the Lyapunov exponent associated with the change of the biomass of the top predator. It appears that the region in the control parameter space where a predator can invade increases with its growth rate. The resulting system becomes more resistant to further invasion when the top predator grows faster. This implies that short food chains with moderate growth rate of the top predator are liable to be invaded by fast growing invaders which consume the top predator. There may be, however, biological constraints on the top predator's growth rate. Predators are generally larger than prey while larger organisms commonly grow slower. As a result, the growth rate generally decreases with the trophic level. This may enable short food chains to be resistant to invaders. We will relate these results to ecological community assembly and the debate on the length of food chains in nature. 

*Keywords:* Bifurcation diagram; Chemostat; Community assembly; Food chain; Invasion of top predator

* Corresponding author. Tel.: +31-20 444 7129, fax: +31-20 444 7123; e-mail: kooi@bio.vu.nl

0025-5564/99/$ – see front matter 
PII: S0025-5564(98)10083-4

## 1. Introduction

Food chains in the chemostat with an abiotic substrate at the base are studied in this paper. Population dynamics at each trophic level follows the Dynamic Energy Budget (DEB) model [1]. This model takes energy reserves into account, leading to an additional state variable besides the population biomass. Ingested food is converted into energy which is added to the energy reserves. From this pool, energy is used for maintenance and growth. The derivation of the population dynamic model from the dynamics of the individuals, which propagate by binary fission, is discussed in Ref. [2].

Cunningham and Nisbet [3], and Nisbet et al. [4] studied the dynamic behaviour of a two-trophic microbial food chain consisting of substrate, bacterium and ciliate in a chemostat. They showed that the introduction of maintenance has a stabilizing effect, especially at low dilution rates. In Refs. [5–7], a study is made of the complex dynamics of a forced two-trophic microbial food chain in a chemostat, driven by a periodic inflow of substrate. This forced system displays quasi-periodicity, phase locking, period doubling and chaotic dynamical behaviour.

The aim of this paper is to study invasion by a top predator into microbial food chains in the chemostat. Furthermore, bifurcation diagrams for food chains of length three and four are discussed. These diagrams describe the dynamic behaviour of the invaded system. For chemostats, the dilution rate and the concentration of the substrate in the reservoir are the natural free bifurcation parameters. These are the control parameters of the chemostat which are set by the experimentalist. Consequently, all points in the bifurcation diagrams are for a fixed composition of the food chain. The diagram for the three-trophic food chain resembles those of the so-called Rosenzweig–MacArthur model [8,9], for ecosystems [10–14]. Various types of complex dynamics, including chaotic behaviour, are found.

We will relate the results to the debate on the length of food chains in nature. Yodzis [15] and Post and Pimm [16] among others dealt with invasion of a species in a community. In these studies it is assumed that the invaded system converges to a stable equilibrium; a situation which holds for the Lotka–Volterra model with a linear functional response. However, models with the Holling type II, that is a hyperbolic functional response, such as the present DEB model, multiple attractors for certain regions in the free parameter space exist. Furthermore, besides point attractors, limit cycles and strange attractors can occur. The presence of these attractors complicates the study of the invasion by a top predator considerably.

The paper is organized as follows. In Section 2 the model is described. In Section 3 bifurcation diagrams for food chains of different lengths are presented. The set of parameter values proposed in Ref. [3] is used. Only local

bifurcations will be dealt with. The results were obtained using different general-purpose bifurcation computer software packages AUTO [17,18], and LOCBIF, CONTENT [19,20] supplemented with special purpose codes written by ourselves.

Section 4 deals with the resistance of a food chain to invasion by a top predator. A top predator invades when it is able to increase after the introduction of a small number of individuals in a food chain. The condition for invasion of a top predator is proven to be identical to the condition for transcritical bifurcations in the case of equilibria, limit cycles and chaos. For an increasing maximum growth rate of the top predator, the resistance of the food chain to invasion decreases and simultaneously the resistance of the food chain after invasion increases. These results suggest that there are also severe restrictions on the existence of short food chains with moderate maximum growth rate of its top predator. In Section 5 we will relate these observations to the assembly community method and to hypotheses on the length of food chains in nature, as proposed in the literature.

## 2. The model

The chemostat is a well-stirred vessel with constant influx of the substrate, $x_r$ and out flux with dilution rate, $D$. Let $x_0(t)$ denote the density of the resource (substrate) and let $x_i(t)$, $i = 1, \ldots, n$, denote the biomass densities of prey, any number of intermediate predators, and, finally, the top predator, where $n$ is the number of trophic levels. Furthermore, let $e_i(t)$, $i = 1, \ldots, n$, denote the scaled reserve densities. At each trophic level, the scaled energy density is defined as the actual energy density divided by the maximum energy density, which is assumed to be a species-specific parameter. The model reads

$$\frac{\mathrm{d}x_0}{\mathrm{d}t} = (x_r - x_0)D - I_{0,1}x_1 f_{0,1}(x_0), \tag{1a}$$

$$\frac{\mathrm{d}e_i}{\mathrm{d}t} = v_{i-1,i}(f_{i-1,i}(x_{i-1}) - e_i), \quad i = 1, \ldots, n, \tag{1b}$$

$$\frac{\mathrm{d}x_i}{\mathrm{d}t} = (\mathscr{M}_{i-1,i}(e_i) - D)x_i - I_{i,i+1}x_{i+1}f_{i,i+1}(x_i), \quad i = 1, \ldots, n-1, \tag{1c}$$

$$\frac{\mathrm{d}x_n}{\mathrm{d}t} = (\mathscr{M}_{n-1,n}(e_n) - D)x_n, \tag{1d}$$

where the scaled Holling type II functional response $f_{i-1,i}$ is defined by

$$f_{i-1,i}(x_{i-1}) \stackrel{\text{def}}{=} \frac{x_{i-1}}{k_{i-1,i} + x_{i-1}}, \quad i = 1, \ldots, n, \tag{2}$$

and the growth rate $\mathscr{M}_{i-1,i}$ by

$$\mathscr{M}_{i-1,i}(e_i) \overset{\text{def}}{=} \frac{v_{i-1,i}e_i - m_i g_i}{e_i + g_i}, \quad i = 1, \ldots, n. \tag{3}$$

The last term on the right-hand sides of Eqs. (1a) and (1c) represents the depletion rate due to predation. This functional response is proportional to the predator biomass density, where the proportionality parameter $I_{i-1,i}$ is the maximum ingestion rate. Two sub-indices are used to indicate that two levels, prey and predator, are involved. The first term on the right-hand sides of Eqs. (1c) and (1d) is the growth term, which is proportional to biomass density. Finally, there are terms due to washout. This term is given as $D_{x_i}$ for all trophic levels. For the top predator this is the only source of depletion. Eq. (1b) is a constitutive relationship which states that the energy reserves density dynamics follows food dynamics via a first order process. This equation is defined at the individual level. It is assumed that all individuals belonging to the population possess the same reserve energy density. Eq. (1b) is not a mass balance equation and therefore there is no washout term. For the biological meaning of the parameters the reader is referred to Ref. [1] and also Table 1.

We now show that the solution of system (1) is bounded. We first observe that the boundaries of the positive cone, $x_i = 0$, for $i = 1, \ldots, n$, are invariant and therefore the biomass densities are positive, $x_i(t) > 0$, $t \geqslant 0$ when $x_i(0) > 0$, because of the uniqueness of the solution. Furthermore, Eq. (1b) imply that $0 \leqslant e_i(t) \leqslant 1$, $t \geqslant 0$ when $0 \leqslant e_i(0) \leqslant 1$, since $0 \leqslant f_{i-1,i}(x_{i-1}(t)) \leqslant 1$. Eq. (1a) shows that for the density of the substrate in the reactor $\mathrm{d}x_0/\mathrm{d}t > 0$ for $x_0 = 0$ and therefore the density of the substrate is non-negative: $x_0(t) \geqslant 0$, $t \geqslant 0$ when $x_0(0) \geqslant 0$.

Finally we introduce dissipated mass densities $p_i$ expressed in the same units as the $x_i$ (for example C-moles)

Table 1
Parameters and state variables ($t$ = time, $m$ = biomass, $v$ = volume of the reactor; the subindex denotes the trophic level)

| Parameter | Dimension | Units | Interpretation |
|---|---|---|---|
| $t$ | $t$ | h | Time |
| $x_0$ | $m\ v^{-1}$ | mg dm$^{-3}$ | Substrate density |
| $x_i$ | $m\ v^{-1}$ | mg dm$^{-3}$ | Biomass density |
| $x_r$ | $m\ v^{-1}$ | mg dm$^{-3}$ | Substrate concentration in reservoir |
| $D$ | $t^{-1}$ | h$^{-1}$ | Dilution rate |
| $k_{i-1,i}$ | $m\ v^{-1}$ | mg dm$^{-3}$ | Saturation constant |
| $I_{i-1,i}$ | $t^{-1}$ | h$^{-1}$ | Maximum food uptake rate |
| $\mu_{i-1,i}$ | $t^{-1}$ | h$^{-1}$ | Overall maximum population growth rate |
| $y_{i-1,i}$ | – | – | Maximum yield |
| $m_i$ | $t^{-1}$ | h$^{-1}$ | Maintenance rate coefficient |
| $v_{i-1,i}$ | $t^{-1}$ | h$^{-1}$ | Energy conductance, $\propto$ assimilation rate |
| $g_i$ | – | – | Energy investment ratio, $\propto$ costs for growth |

$$\frac{dp_1}{dt} = x_1\left(\left(1 - \frac{1}{y_{0,1}}\right)\mu_{0,1}f_{0,1} + m_1\right) - Dp_1, \tag{4a}$$

and for each level $i = 2, \ldots, n$

$$\frac{dp_i}{dt} = x_i\left(\left(1 - \frac{1}{y_{i-1,i}}\right)\mu_{i-1,i}f_{i-1,i} + m_i\right) + x_i\frac{e_{i-1}}{g_{i-1}}I_{i-1,i}f_{i-1,i} - Dp_i, \tag{4b}$$

where we assume that these dissipated masses leave the reactor via the efflux with dilution rate $D$. This washout is represented by the last term on the right-hand sides of Eqs. (4a) and (4b). The first term on the right-hand sides is due to incomplete conversion from biomass of the prey into biomass of the predator. The maximum growth rate is defined by $\mu_{i-1,i} = v_{i-1,i}/g_i$. Then the maximum yield defined by $y_{i-1,i} = \mu_{i-1,i}/I_{i-1,i}$, for $i = 1, \ldots, n$, is smaller than 1 because mass cannot be generated spontaneously. The second term $m_i x_i$ is associated with the costs for maintenance. The third term on the right-hand side of Eq. (4a) is the equivalent biomass which reflects the unused reserve energy stored in the prey because predators do not use the prey energy reserves, $e_{i-1}$, for growth. In a forthcoming paper, the consequences of the latter assumption will be studied.

Eqs. (4a) and (4b) imply, since the first terms are non-negative (all parameter values are positive and $y_{i-1,i} \leqslant 1$, $0 \leqslant f_{i-1,i} \leqslant 1$, $0 \leqslant e_i \leqslant 1$), that $p_i(t) \geqslant p_i(0)\exp(-Dt)$ and hence the dissipated mass densities $p_i$ are non-negative for $t \geqslant 0$ when $p_i(0) > 0$ with $i = 1, \ldots, n$.

The weighted total biomass in the reactor may be defined by

$$H(t) = x_0(t) - x_r + \sum_{i=1}^{n}\left(\frac{e_i}{g_i} + 1\right)x_i(t) + \sum_{i=1}^{n}p_i(t), \quad t \geqslant 0. \tag{5}$$

For this quantity $H(t)$ we have

$$\frac{dH}{dt} = -DH. \tag{6}$$

Therefore, $x_i(t) \geqslant 0$, $i = 0, \ldots, n$ and $p_i(t) \geqslant 0$, $i = 1, \ldots, n$ are bounded for $t \geqslant 0$, and system (1) converges asymptotically to the invariant hyperplane $H = 0$.

## 3. Bifurcation diagrams

The bifurcation parameters are the chemostat control parameters: the dilution rate, $D$, and the concentration substrate in the reservoir, $x_r$. The parameter values together with the unitsystem are given in Table 2. Most bifurcation curves for equilibria as well as the codimension 2 points were calculated with LOCBIF [19,21]. AUTO [18] was used for the calculation of the bifurcation curves for limit cycles, including period doubling.

Due to the parameter values for the prey (namely $g_1 = 80$ and $v_1 = 40$) the full system (1) happens to be stiff. In order to circumvent numerical problems

Table 2
Parameter set for bacterium-ciliate models, after Cunningham and Nisbet [3,4]

| Parameter | Unit | Values | | | |
|---|---|---|---|---|---|
| | | $i=1$ | $i=2$ | $i=3$ | $i=4$ |
| $y_{i-1,i}$ | – | 0.4 | 0.6 | 0.6 | 0.6 |
| $\mu_{i-1,i}$ | $h^{-1}$ | 0.5 | 0.2 | 0.15 | 0.1 |
| $k_{i-1,i}$ | mg $dm^{-3}$ | 8 | 9 | 10 | 20 |
| $I_{i-1,i}$ | $h^{-1}$ | 1.25 | 0.33 | 0.25 | 0.167 |
| $m_i$ | $h^{-1}$ | 0.025 | 0.01 | 0.0075 | 0.005 |
| $g_i$ | – | 80.0 | 1.0 | 0.504 | 0.4 |
| $v_{i-1,i}$ | $h^{-1}$ | 40.0 | 0.2 | 0.0756 | 0.04 |

The values for the new parameters $m_i$ (equal to 5% of maximum growth rate $\mu_{i-1,i}$) and $g_i$ are also given. The relationships $I_{i-1,i} = \mu_{i-1,i}/y_{i-1,i}$ and $\mu_{i-1,i} = v_{i-1,i}/g_i$ hold true for $i = 1, \ldots, n$.

and time-consuming computations when calculating the bifurcation diagram, the dynamics of the energy reserves density of the prey is assumed to be quasi-static; that is $e_1(t) = f_{0,1}(x_0(t))$. In this way the originally seven-dimensional problem is reduced to six dimensions. Comparison of the simulation results for the full and reduced system indicates that for the parameter setting given in Table 2 the reduction is justified.

In Fig. 1 we show the bifurcation diagram for a two-trophic food chain. There are three biologically important regions; a region where the predator goes to extinction, a region where a stable equilibrium exists and region where a stable limit cycle exists.

Fig. 2 gives the bifurcation diagram for a three-trophic food chain. The transcritical bifurcation curves $TC_{e,1}$, $TC_{e,2}$ and $TC_{e,3}$, the tangent bifurcation curve $T_{e,3}$ together with the Hopf bifurcation curves $H_2^-$, $H_{3_2}^-$, $H_{3_1}^-$ and $H_3^+$, were already presented in Ref. [2]. In the present paper the bifurcations of periodic orbits are also discussed.

In the region between $H_2^-$, $H_3^+$ and $H_{3_1}^-$ there is a stable interior equilibrium for the three-trophic food chain. At the supercritical Hopf bifurcation curve $H_{3_1}^-$ this equilibrium becomes unstable and a stable limit cycle was found numerically when changing the free parameters in the regions studied in this paper.

Close to the codimension 2 point $M_1$ the Hopf bifurcation curve is initially supercritical ($H_{3_2}^-$) but becomes subcritical ($H_3^+$) at the Bautin bifurcation point $L$, see Fig. 2. The transcritical curve, $TC_{c,3}$, for limit cycles at the boundary of the positive cone with $x_3 = 0$, intersects the Hopf bifurcation curve $H_{3_2}^-$ near point $M_1$. Observe that there is a tangent bifurcation curve for interior limit cycles which orginates in the Bautin bifurcation point $L$ and which is tangent to the transcritical curve $TC_{c,3}$ where it lies on the boundary of the positive cone

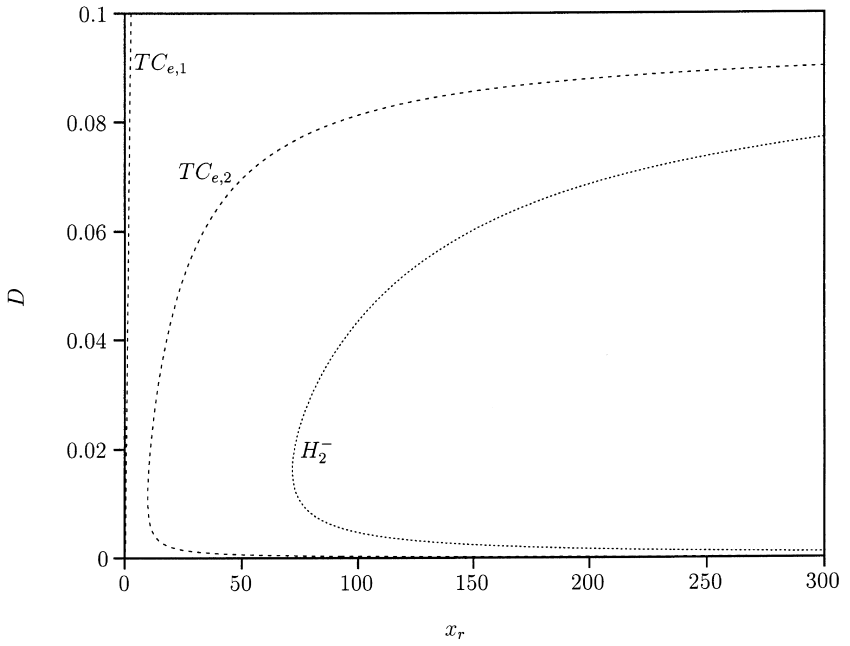


Fig. 1. Bifurcation diagram for DEB model with two trophic levels: system (1) with $n = 2$. Values assigned to physiological parameters are listed in Table 2. The curves $TC_{e,1}$ and $TC_{e,2}$ are transcritical bifurcation curves and $H_2^-$ marks a supercritical Hopf bifurcation curve.

with $x_3(t) = 0$. This tangent bifurcation curve is not displayed in Fig. 2. The dynamics in the region around point $M_1$ was described elsewhere [22].

At the codimension 2 point $M_2$ the transcritical bifurcation for equilibria $TC_{e,3}$ changes from subcritical to supercritical. A tangent bifurcation curve for equilibria $T_{e,3}$ originates in this point $M_2$. Similarly, at the codimension 2 point $M_3$ the transcritical bifurcation for limit cycles $TC_{c,3}$ changes from subcritical to supercritical. In this point $M_3$ a tangent bifurcation curve for limit cycles $T_{c,3_1}$ originates. There is a second tangent bifurcation curve $T_{c,3_2}$ for limit cycles. Curves $F_1$ and $F_2$ mark period-1 $\rightarrow$ 2 flip bifurcations.

Fig. 3 is a one-parameter bifurcation diagram for the local maxima of the top predator $x_3$. The free parameter is the dilution rate $D$ while the concentration substrate in the reservoir is fixed at $x_r = 275$. In order to get rid of the transients, integration is performed for a fixed time (we used 20 000 h) without examination of the results. From that point in time (until 30 000 h) the biomass of the top predator peak value is shown as a dot in the diagram. At the top the rotated bifurcation diagram, Fig. 2, for $250 \leqslant x_r \leqslant 275$ is plotted. Bifurcation points (the $D$ values for intersection points in two-parameter diagram, Fig. 2, of bifurcation curves with $x_r = 275$ line) are indicated by vertical lines in the one-parameter bifurcation diagram Fig. 3.

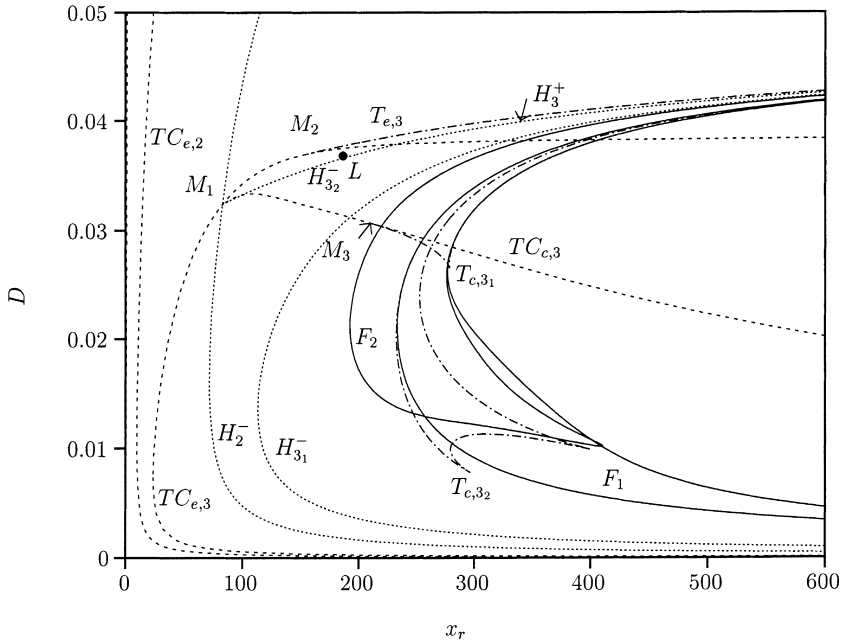


Fig. 2. Bifurcation diagram for DEB model with three levels: system (1) with $n = 3$. Dotted curves $H_3^+$ and $H_3^-$ mark Hopf bifurcations, curve $T_{e,3}$ a tangent bifurcation curve $TC_{e,3}$ marks transcitical bifurcations and curve $TC_{c,3}$ a transcritical bifurcation for limit cycles with $x_3 = 0$. Point $L$ is a Bautin bifurcation point, where the Hopf bifurcation changes from supercritical to subcritical. The solid curves $F_1$ and $F_2$ are flip bifurcations for limit cycles (period-1 $\rightarrow$ 2).

There is a cascade of period doubling which leads to complex dynamic behaviour. The chaotic attractor disappears when $D \approx 0.027$ when an unstable limit cycle cuts the chaotic attractor. With $D \approx 0.0125$ this happens when a limit cycle becomes unstable itself at a tangent bifurcation (curve $T_{c,3_1}$). In Ref. [23] these boundary crises are studied and linked to global bifurcations.

Fig. 4 shows the two coexisting stable interior limit cycles together with the unstable limit cycle on the boundary of the positive cone for $D = 0.01$ and $x_r = 275$. The arrow gives the direction in which the orbit is traversed. The dot in the middle is the position of the unstable equilibrium, a saddle point with a pair of complex conjugated eigenvalues with positive real part. One of the displayed stable limit cycles passes the unstable positive equilibrium closely, indicating the possibility of the homoclinic orbit. In Ref. [24] we found a global Shil'nikov homoclinic bifurcation (Ref. [21], p. 204) for the unstable positive equilibrium for $D \approx 0.015$.

In Fig. 5 we show the bifurcation diagram for a four-trophic food chain. The parameter values are given in Table 2. This diagram shows some similarities with the diagram for the three-trophic food chain (Fig. 2) in the

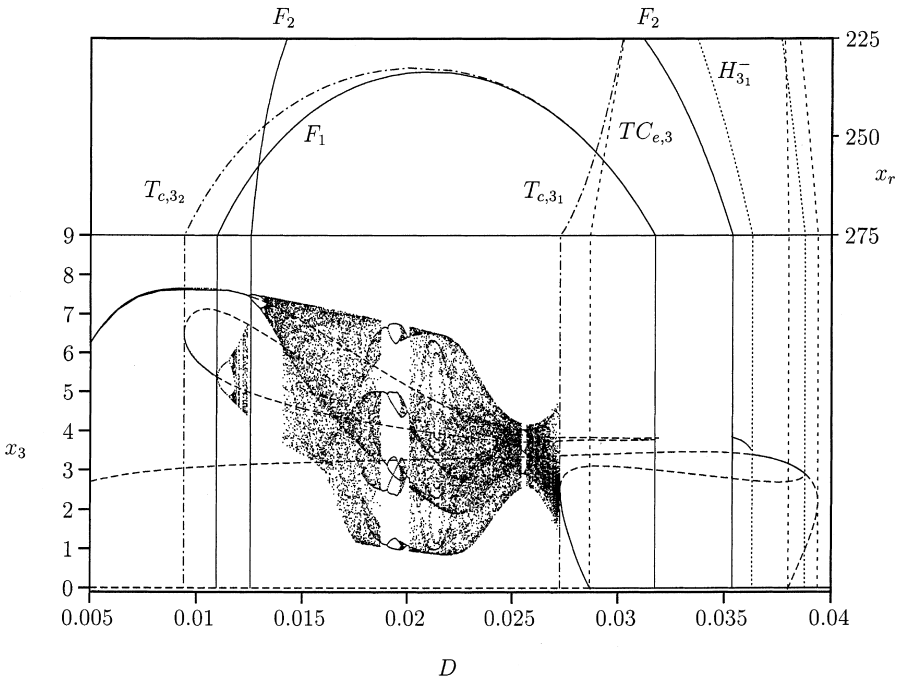


Fig. 3. One-parameter bifurcation diagram for peak values of top predator as a function of dilution rate $D$, where concentration in reservoir is $x_r = 275$ mg dm$^{-3}$. Solid curve gives stable equilibrium values while dashed curve shows unstable equilibrium values. The dashed curves are unstable attractors. At the top the rotated two-parameter bifurcation diagram, Fig. 2, for $250 \leqslant x_r \leqslant 275$ mg dm$^{-3}$ is plotted. Bifurcation points (the $D$ values for intersection points in two-parameter diagram, Fig. 2, of bifurcation curves with $x_r = 275$ line) are indicated by vertical lines in the one-parameter bifurcation diagram.

neighbourhood of the codimension 2 point $M_1$, which is now on the supercritical Hopf bifurcation curve for the three-trophic food chain $H_3^-$. This point also lies on the transcritical curve for equilibria $TC_{e,4}$ and in this point a supercritical Hopf bifurcation $H_{4_2}^-$ originates which becomes subcritical, curve $H_4^+$, in the Bautin bifurcation point $L_1$ and later supercritical, curve $H_{4_1}^-$, again in the point $L_2$. From these points there originate again tangent bifurcation curves for limit cycles denoted by $T_{c,4_1}$ and $T_{c,4_2}$. Finally, from $M_1$ also transcritical bifurcation for limit cycles occurs, curve $TC_{c,4}$. As in the case of a three-trophic level food chain from $M_2$, where it becomes supercritical, a tangent bifurcation curve for equilibria $T_{e,4}$ originates. Only period-1 $\rightarrow$ 2 flip bifurcations curves $F_1$ and $F_2$ are shown. In the region inside these curves complex dynamic behaviour can occur, but this is not discussed in this paper.

The transcritical curves for equilibria $TC_{e,3}$ and $TC_{e,4}$ and for limit cycles $TC_{c,3}$ and $TC_{c,4}$ for the three- and four-trophic food chain, displayed in Figs. 2

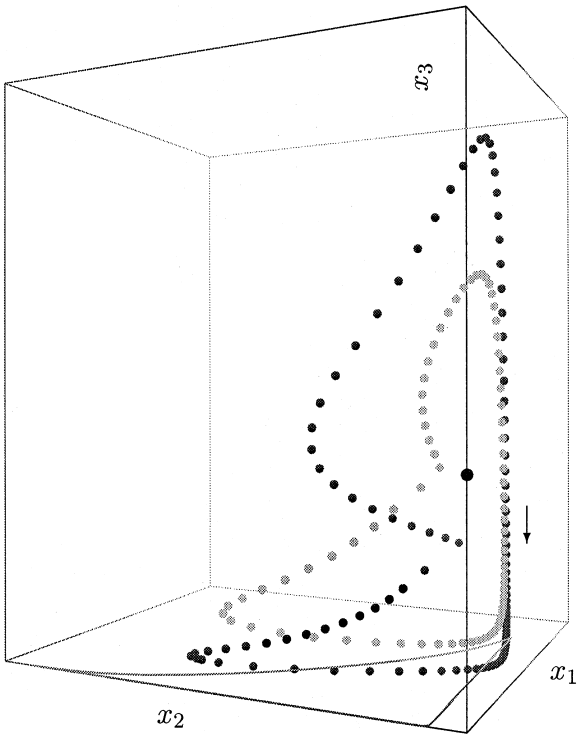


Fig. 4. Phase portrait simulation with DEB model for dilution rate $D = 0.01\ \mathrm{h}^{-1}$ and concentration in the reservoir $x_r = 275\ \mathrm{mg\ dm}^{-3}$. The ranges for the three variables are $0 \leqslant x_1 \leqslant 100\ \mathrm{mg\ dm}^{-3}$, $0 \leqslant x_2 \leqslant 30\ \mathrm{mg\ dm}^{-3}$ and $0 \leqslant x_3 \leqslant 9\ \mathrm{mg\ dm}^{-3}$. Two interior stable limit cycles and one unstable limit cycle with $x_3 = 0$ on the boundary of the phase space. The dots are equidistant in time with time separation of 4.0 h. On the bottom plane the stable limit cycle for the two-trophic food chain is plotted. The large dot denotes the unstable positive equilibrium. The arrow gives the direction of the flow.

and 5 are important with respect to the invasibility of a top predator, as will be explained in the next section.

## 4. Invasibility of a top predator

Invasion via a point attractor, limit cycle and finally chaotic attractor will now be discussed. The area in the $x_r$, $D$-plane where invasion is possible will be used as a measure for invasibility. Sensitivity with respect to the maximum growth rate of the top predator is analysed at the end of this section.

Let $n$ be the length of the food chain with the potential invader included as the top predator. The region of persistence of the food chain is bounded by two

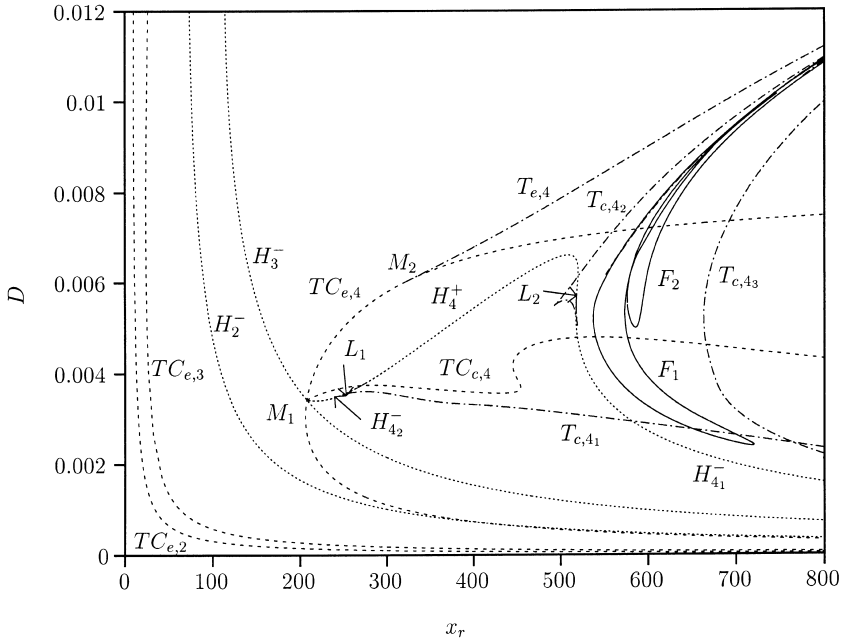


Fig. 5. Bifurcation diagram for DEB model with four trophic levels: system (1) with $n = 4$. Point $M_1$ is intersection point for $TC_{e,4}$, $H_3^-$, $H_{4_2}^-$, $TC_{c,4}$. The curves $TC_{e,4}$ and $TC_{c,4}$ are transcritical bifurcation curves for the equilibria and limit cycles, respectively and $H_{4_1}^-$, $H_{4_2}^-$ and $H_4^+$ mark supercritical and one subcritical Hopf bifurcation curve, respectively. Point $M_2$ is the intersection of the transcritical bifurcation curve $TC_{e,4}$ and the tangent bifurcation curve $T_{e,4}$, both for equilibria. Points $L_1$ and $L_2$ are Bautin bifurcation points, where the Hopf bifurcation changes from supercritical to subcritical and backward. From these points $L_1$ and $L_2$ tangent bifurcation curves for limit cycles, $T_{c,4_1}$ and $T_{c,4_2}$ originate. The solid curves $F_1$ and $F_2$ are flip bifurcations for limit cycles (period-1 $\rightarrow$ 2).

transcritical bifurcation curves; $TC_{e,n}$ for the equilibria, and $TC_{c,n}$ for the limit cycles. In order to investigate invasion the stability of the attractor on the boundary of the positive cone, where $x_j(t) > 0$, $j < n$ and $x_n(t) = 0$, has to be considered as part of the $n$-trophic food chain. These attractors are stable with respect to the $(n-1)$-trophic food chain. Our technique is a variation on the procedure worked out in Ref. [25].

We start with invasion of a boundary equilibrium which is assumed to be stable. For example, on the left side of the Hopf bifurcation curve $H_2^-$ in Fig. 1, the stable equilibrium of the $(n-1)$-trophic food chain is denoted by

$$E_0 = (\bar{x}_0\ \bar{e}_1\ \bar{x}_1\ \cdots\ \bar{e}_{n-1}\ \bar{x}_{n-1}\ \bar{e}_n\ \bar{x}_n)^{\mathrm{T}}, \tag{7}$$

where $\bar{x}_n = 0$ and $\bar{e}_n = f_{n-1,n}(\bar{x}_{n-1})$. Let $\mathscr{I}$ be the $(2n-1) \times (2n-1)$ Jacobian matrix for the $(n-1)$-trophic food chain and $\mathscr{J}$ be a $(2n+1) \times (2n+1)$ Jacobian matrix for the $n$-trophic food chain, both evaluated at $E_0$

$$\mathscr{J} = \begin{pmatrix} & & & & 0 & 0 \\ & & \mathscr{I} & & \vdots & \vdots \\ & & & & 0 & 0 \\ & & & & 0 & -I_{n-1,n}\bar{f}_{n-1,n} \\ 0 & \dots & 0 & v_{n-1,n}\bar{f}'_{n-1,n} & -v_{n-1,n} & 0 \\ 0 & \dots & 0 & 0 & 0 & \bar{\mathscr{M}} - D \end{pmatrix}, \tag{8}$$

where $\bar{f}_{n-1,n} = f_{n-1,n}(\bar{x}_{n-1})$ and

$$\bar{f}'_{n-1,n} = \frac{\mathrm{d}f_{n-1,n}}{\mathrm{d}x_{n-1}}(\bar{x}_{n-1})$$

and the actual growth rate of the top predator $\bar{\mathscr{M}} = \mathscr{M}_{n-1,n}(\bar{e}_n)$.

Expanding the determinant of matrix $\mathscr{J} - \lambda I$, where $I$ is the $(2n+1) \times (2n+1)$ identity matrix we find

$$\det(\mathscr{J} - \lambda I) = \det(\mathscr{I} - \lambda I) \times (-v_{n-1,n} - \lambda) \times (\bar{\mathscr{M}} - D - \lambda). \tag{9}$$

Hence, besides the $2n-1$ eigenvalues with negative real parts (by assumption of a stable equilibrium $E_0$ of the $(n-1)$-trophic food chain) of the matrix $\mathscr{I}$, there are two additional eigenvalues, namely $-v_{n-1,n}$, which is always negative, and $\bar{\mathscr{M}} - D$.

The zero-crossing of the latter expression thus turns out to be the test-function for the transcritical bifurcation $TC_{e,n}$. In these points the growth rate of top predator $\bar{\mathscr{M}}$ equals just the depletion rate $D$. When the growth rate $\bar{\mathscr{M}}$ is greater than the depletion rate $D$ the equilibrium $E_0$ becomes unstable. As a result the top predator can invade. Hence the invasibility condition reads $\bar{\mathscr{M}} > D$.

We now restrict our attention to a three-trophic food chain, $n = 3$ whose bifurcation diagram is given in Fig. 2. The values for the state variables in equilibrium will be taken as functions of the two control parameters $D$ and $x_r$. The function $\bar{\mathscr{M}} - D$ is zero on the curves $TC_{e,3}$ and its partial derivative with respect to $x_r$ is positive for all $x_r$ as will be derived below. In the equilibrium point $E_0$, the right-hand sides of system (1) are zero and we have $\bar{x}_3 = 0$ and $\bar{e}_i = \bar{f}_{i-1,i}$ for $i = 1, 2, 3$. It is easy to show that

$$\frac{\mathrm{d}f_{2,3}(\bar{x}_2)}{\mathrm{d}\bar{x}_2} > 0, \tag{10}$$

and therefore

$$\frac{\mathrm{d}(\mathscr{M}(f_{2,3}(\bar{x}_2)) - D)}{\mathrm{d}\bar{x}_2} > 0. \tag{11}$$

Because $\bar{x}_3 = 0$, Eq. (1c) for $i = 2$ gives an expression for $\bar{x}_i$ which is independent of $x_r$. Then, from Eq. (1a) it follows that $\partial\bar{x}_0/\partial x_r > 0$ and subsequently from Eq. (1c) with $i = 1$ that $\partial\bar{x}_2/\partial x_r > 0$. Together with Eq. (11) we conclude that $\partial(\bar{\mathscr{M}} - D)/\partial x_r > 0$ for the whole region bounded by the curves $TC_{e,3}$ and $H_2^-$ and consequently in that region we have $\bar{\mathscr{M}} - D > 0$; that is, the top predator can invade.

The stability of the boundary limit cycles (for example for $n = 3$ on the right side of the Hopf bifurcation curve $H_2^-$ in the bifurcation diagram Fig. 2), denoted by

$$L_0(t) = (\tilde{x}_0(t)\ \tilde{e}_1(t)\ \tilde{x}_1(t)\ \cdots\ \tilde{e}_{n-1}(t)\ \tilde{x}_{n-1}(t)\ \tilde{e}_n(t)\ \tilde{x}_n(t))^{\mathrm{T}}\ , \tag{12}$$

will now be studied. We have $\tilde{x}_n(t) = 0$ and the function $\tilde{e}_n(t)$ is the solution of the linear ODE (1b) for $i = n$ with a periodic coefficient $\tilde{f}_{n-1,n}(t)$

$$\frac{\mathrm{d}\tilde{e}_n}{\mathrm{d}t} = v_{n-1,n}\left(\tilde{f}_{n-1,n}(t) - \tilde{e}_n\right), \tag{13}$$

and a periodic boundary condition $\tilde{e}_n(0) = \tilde{e}_n(T_0)$. We assume that this periodic orbit with period $T_0$ is stable for the $(n-1)$-trophic food chain.

Let $\mathscr{I}(t)$ now be a $(2n-1) \times (2n-1)$ continuous periodic matrix of period $T_0$ and $\Psi(t)$ the fundamental matrix of $\dot{y} = \mathscr{I}(t)y$, where

$$y(t) = \begin{pmatrix} x_0(t) - \tilde{x}_0(t) \\ e_1(t) - \tilde{e}_1(t) \\ x_1(t) - \tilde{x}_1(t) \\ \vdots \\ e_{n-1}(t) - \tilde{e}_{n-1}(t) \\ x_{n-1}(t) - \tilde{x}_{n-1}(t) \end{pmatrix}. \tag{14}$$

Let $\mathscr{J}(t)$ denote the $(2n+1) \times (2n+1)$ periodic matrix of the form

$$\mathscr{J}(t) = \begin{pmatrix} & & & 0 & 0 \\ & \mathscr{I}(t) & & \vdots & \vdots \\ & & & 0 & 0 \\ & & & 0 & -I_{n-1,n}\tilde{f}_{n-1,n}(t) \\ 0 \ \ \ldots \ \ 0 & v_{n-1,n}\tilde{f}'_{n-1,n}(t) & & -v_{n-1,n} & 0 \\ 0 \ \ \ldots \ \ 0 & 0 & & 0 & \tilde{\mathscr{M}}(t) - D \end{pmatrix}, \tag{15}$$

where $\tilde{f}_{n-1,n} = f_{n-1,n}(\tilde{x}_{n-1})$, $\tilde{f}'_{n-1,n} = (\mathrm{d}f_{n-1,n}/\mathrm{d}x_{n-1})(\tilde{x}_{n-1})$ and for the instantaneous actual growth rate of the top predator $\tilde{\mathscr{M}}(t) = \mathscr{M}_{n-1,n}(\tilde{e}_n(t))$. Then with initial condition $\Phi(0) = I$ and where

$$z(t) = \begin{pmatrix} y(t) \\ e_n(t) - \tilde{e}_n(t) \\ x_n(t) - \tilde{x}_n(t) \end{pmatrix}, \tag{16}$$

the fundamental matrix $\Phi(t)$ of $\dot{z} = \mathscr{J}(t)z$ is given by

$$\Phi(t) = \begin{pmatrix} & & & 0 & \eta_1(t) \\ & \Psi(t) & & \vdots & \vdots \\ & & & 0 & \eta_{2n-2}(t) \\ \zeta_1(t) & \ldots & \zeta_{2n-2}(t) & \exp\{-v_{n-1,n}t\} & \eta_{2n-1}(t) \\ 0 & \ldots & 0 & 0 & \exp\{\int_0^t (\tilde{\mathscr{M}} - D)\,\mathrm{d}\tau\} \end{pmatrix}. \tag{17}$$

All functions are evaluated along the periodic orbit $L_0$. The functions $\zeta_i(t)$ and $\eta_i(t)$, where $i = 1, \ldots, 2n-1$, are given by ODES, which are not formulated here. Any solution $z(t)$ satisfies

$$z(T_0) = \Phi(T_0)z(0). \tag{18}$$

By assumption of a stable periodic orbit of the $(n-1)$-trophic cycle $L_0$, one eigenvalue of the matrix $\Psi(T_0)$ is equal to 1 and the other eigenvalues $2n-2$ are inside the unit cycle. Expanding the determinant of the monodromy matrix $\Phi(T_0)$ of the cycle $L_0$ we find that besides $2n-1$ eigenvalues of $\Psi(T_0)$ there are two additional Floquet multipliers, eigenvalues of $\Phi(T_0)$, namely $\exp\{-v_{n-1,n}T_0\}$, which always lies inside the unit circle, and $\exp\{\int_0^{T_0} \tilde{\mathscr{M}}(t)\,\mathrm{d}t - T_0 D\}$. When this second multiplier equals 1 the mean growth rate of the top predator equals just the depletion rate $D$. The invasibility condition reads

$$T_0^{-1} \int_0^{T_0} \tilde{\mathscr{M}}(t)\,\mathrm{d}t > D. \tag{19}$$

Finally we study invasion when the $(n-1)$-trophic food chain shows chaotic behaviour. One route to chaotic behaviour is via a cascade of period doubling (Fig. 3) where $T_0$ increases to infinity. This cascade suggests that the condition for invasion is just Eq. (19) with $T_0 \to \infty$ where we integrate along the aperiodic chaotic attractor, denoted by

$$C_0(t) = (\hat{x}_0(t)\ \hat{e}_1(t)\ \hat{x}_1(t)\ \cdots\ \hat{e}_{n-1}(t)\ \hat{x}_{n-1}(t)\ \hat{e}_n(t)\ \hat{x}_n(t))^{\mathrm{T}}, \tag{20}$$

where $\hat{x}_n = 0$ and where the energy density $\hat{e}_n$ is the solution of the following ODE

$$\frac{\mathrm{d}\hat{e}_n}{\mathrm{d}t} = v_{n-1,n}(\hat{f}_{n-1,n}(t) - \hat{e}_n), \tag{21}$$

with $\hat{f}_{n-1,n}(t) = f_{n-1,n}(\hat{x}_{n-1}(t))$. By assumption the system is initially (at $t = 0$) in the basis of attraction of the strange attractor $C_0$.

In order to derive the invasibility condition we use the notion of the Lyapunov exponent. Because the $(n-1)$-trophic food chain is chaotic at least, one of its Lyapunov exponents is positive. As in the case of the boundary equilibria $E_0$ and the limit cycles $L_0$, two Lyapunov exponents associated with the top predator are independent from those of the invaded system. The determinant of the Jacobian matrix can therefore be factorized as in Eq. (9). This is due to an important feature of the Jacobian matrices $\mathscr{J}$ and $\mathscr{J}(t)$ given in Eqs. (8) and (15). The element $\mathscr{J}_{2n-1,2n}$ is zero, as a result of the requirement that both factors $\mathscr{M}(e_n) - D$ and $x_n$ on the right-hand side of Eq. (1d) are zero. In food chains, the top predator consumes only the predator and hence the elements $\mathscr{J}_{2n,i}$, $i = 1, \ldots, 2n-2$, on the last row are zero too. For the same

reason the first $2n-1$ elements of column $2n-1$ elements $\mathscr{J}_{j,2n-1}$, $j = 1,\ldots,2n-1$ are zero as well.

The Lyapunov exponent evaluated for the boundary attractor with $x_n = 0$ is defined by (see Ref. [26])

$$\lim_{T\to\infty} T^{-1} \int_0^T \frac{1}{x_n} \frac{\mathrm{d}x_n}{\mathrm{d}t}\, \mathrm{d}t = \lim_{T\to\infty} T^{-1} \int_0^T (\hat{\mathscr{M}}(t) - D)\, \mathrm{d}t, \tag{22}$$

where $\hat{\mathscr{M}}(t) = \mathscr{M}(\hat{e}_n(t))$ is the growth rate function evaluated on the boundary chaotic attractor $C_0$. The top predator can invade when this Lyapunov exponent is positive.

Now we consider a three-trophic food chain again. Below the bifurcation curve $TC_{e,3}$ in Fig. 2 the mean growth rate is greater than the depletion rate $D_3$ and the periodic orbit $L_0$ becomes unstable. In that region the multiplier associated with the biomass of the top predator is greater than 1. As a result the top predator can invade in this region.

The position in the bifurcation diagram determines to which attractor the system will converge when a small perturbation of the unstable equilibrium or limit cycle on the boundary attractor of the positive cone is applied. With invasion of a two-trophic food chain the system will converge asymptotically to a unique positive point attractor of the resulting three-trophic chain regardless of whether the two-trophic food chain is originally in a point attractor or a limit cycle. The top predator controls the oscillating two-trophic food chain towards a stable interior equilibrium, namely when $H_3^-$ is on the left side of $H_2^-$.

Finally the influence of the maximum growth rate of the top predator on the resistance of a two-trophic food chain to invasion may be studied. To that end the codimension 2 bifurcation point $M_1$ in Fig. 2 is continued with three bifurcation parameters, $D$, $x_r$ and $v_{2,3}$. In order to assess the invasibility of the resulting invaded system the influence of the maximum growth rate of the predator is also studied. Then the three bifurcation parameters are $D$, $x_r$ and $v_{1,2}$. We took in all cases the maintenance rate to be 5% of the maximum growth rate; that is $m_i = 0.05\mu_{i-1,i}$. All other parameters given in Table 2 are kept constant.

Fig. 6 shows the bifurcation diagram for these cases. There is a stable equilibrium for the two-trophic food chain in the region bounded by the two transcritical bifurcation curves $TC_{e,2}$ and $TC_{e,3}$. When $\mu_{1,2} = 0.5$ the invasibility region of the top predator is smaller than in the original case with $\mu_{1,2} = 0.2$. When $\mu_{2,3} = 0.2$ the region with resistance to invasibility is much smaller than in the original case. This shows that a potential invader with a high maximum growth rate can invade easily and subsequently that a high maximum growth rate of the invaded top predator gives a high resistance to further invasion of the food chain.

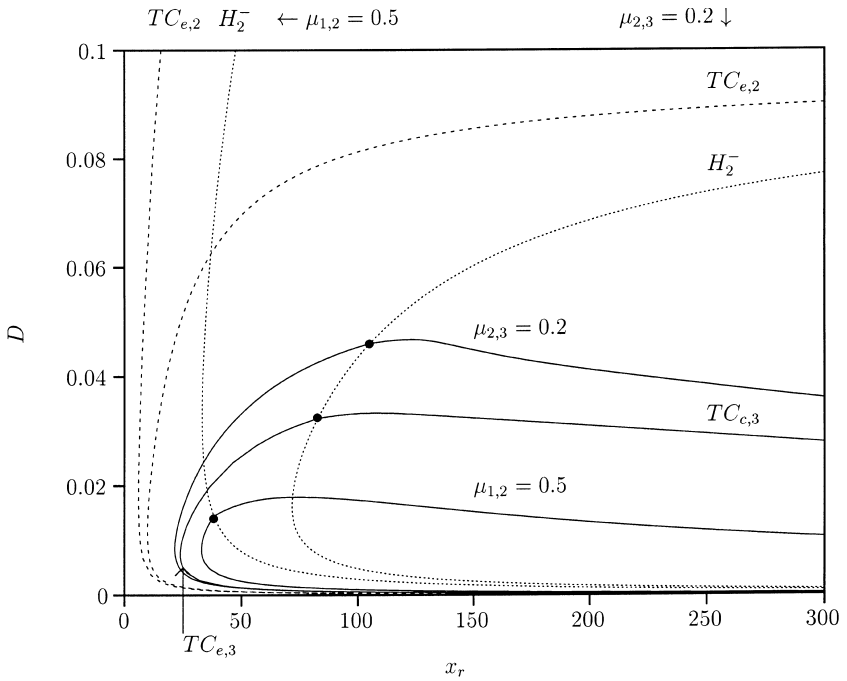


Fig. 6. Bifurcation diagram for DEB model, system (1), for three cases, parameter setting given in Table 2, large growth rate for the predator ($\mu_{1,2} = 0.5$ h$^{-1}$ instead of 0.2 h$^{-1}$) and larger growth rate for the top predator ($\mu_{2,3} = 0.2$ h$^{-1}$ instead of 0.15 h$^{-1}$). For an explanation of the symbols see Fig. 2. With maximum growth rate of the top predator $\mu_{2,3} = 0.2$ h$^{-1}$ the bifurcation curves $H_2^-$ and $TC_{e,2}$ are those for the original diagram. The dots are the codimension 2 point $M_1$ for the three cases.

## 5. Discussion and conclusions

Yodzis ([15], p. 231) formulates three criteria which need to be satisfied for a successful invasion of a species in a community when there is a unique positive equilibrium point:

1. A colonizing species must be able to increase when rare.
2. When the new species is added to the community, there must be an equilibrium with at least one positive density.
3. That equilibrium must be locally stable.

Post and Pimm [16] found that in sequences of 200 attempted invasions, two things tended to happen as a community was built up: the return time of the equilibrium increased (lower resilience) and it became more difficult for new species to invade (invasion resistance). The Lotka–Volterra model was used in their study. For this model the equilibria are the solutions of a linear set of equations (because of the linear functional response), see for instance Ref. [27], p. 59. As a result the conditions mentioned above can be readily checked.

Later, similar studies were also performed based on the Lotka–Volterra dynamics in Refs. [28,29], however in Ref. [30] a number of shortcomings of the technique used in Refs. [16,28] are discussed.

Using Holling type II functional responses complicates the analysis because there are possibly multiple equilibria. In Section 4 a condition is derived that ascertains that after a perturbation of the boundary equilibrium, limit cycle or chaotic attractor, the biomass of the top predator increases but the approach used here leaves unanswered the question to which attractor the invaded system converges.

Eq. (6) shows that system (1) is bounded and dissipative for positive dilution rates, $D > 0$ and positive concentration of substrate in the reservoir, $x_r > 0$, and therefore there is at least one attractor. Introduction of a infinitesimal small amount of top predator results in convergence to the attractor in whose basin of attraction the food chain starts. When the invasibility condition is fulfilled this will be another attractor than the boundary attractor itself. With food chains with more than two-trophic levels, multiple attractors also occur on the boundary and the invasibility condition has to be checked for each boundary attractor separately. With the control parameter setting used in Fig. 4 there are two stable limit cycles and one unstable limit cycle as is clear from Fig. 3 with $D = 0.01$. In that case, it could occur that this system is invasible via one boundary attractor but that the top predator goes into extinction by convergence to another boundary attractor, see also Ref. [31]. The flow passes the unstable boundary attractor via the interior of the positive cone.

To rule out stochastic effects the 'law of large numbers' may be involved. Stochasticity is nevertheless important in the early phase of the invasion. For instance, the founder individual might leave the reactor due to wash out before it can reproduce. To circumvent this situation the volume of the reactor can be increased such that the number of individuals remains large while the biomass density is small. When a top predator immigrates with large densities the model has to be altered, by introduction of an extra positive term on the right-hand side of Eq. (1d) or as an initial state where the biomass density of the top predator is not infinitesimally small. For instance, starting close to the interior equilibrium of the three-trophic food chain with $x_r = 275$ and $D \approx 0.0375$ (Fig. 3) the food chain converges to that equilibrium, while for small initial values for $x_3$ the food chain converges to the stable boundary limit cycle, that is the top predator goes into extinction.

The model predicts that a top predator with a large growth rate can invade a food chain easily, that is for various environmental conditions. If the procedure proposed by Post and Pimm would be followed and the range of possible values for the maximum growth rates is unbounded we would expect that our system does become invasion resistant when a predator with a very high growth rate has invaded. This poses the following question, Why do short food chains with moderate growth rates of the top predator exist at all?

It is tempting to interpret this issue for food chains in nature. Competition in food webs and time-varying (seasonal) environments as they occur in communities in nature are not considered although they will be important factors. On the other hand food chains under chemostat conditions might resemble some ecosystems, for instance when the supply of resources is constant in a very simple model for a lake, see also Ref. [32].

In ecological literature the question, Why are food chains so short?, is discussed frequently, see for instance Refs. [15,32,33]. Empirical evidence indicates that in nature the number of trophic levels within ecosystems seldom exceeds five or six (Ref. [32], p. 142). A number of hypotheses have been proposed to explain this. One hypothesis is based on energy limitation and a second on dynamic properties, namely longer food chains have lower resilience (a measure of the rate at which the ecosystem can recover from disturbances) than shorter chains have. Hutchinson [33] has pointed out that since predators tend to be larger than their prey, predators will get bigger and bigger as one moves up a food chain, so that eventually a further link in the chain would require an animal that is too large to be practical (see Ref. [15], p. 243).

Related ideas are used to address the question raised above, namely that there is no invasion resistance when the growth rate of the invader is very large, an assertion based on the model predictions. To that end individual growth and reproduction rates have to be linked to the population growth rate. In structured population models one distinguishes between members of the population with respect to age or size. The dynamics is mathematically described by a partial differential equation. Several techniques have been developed (see Refs. [34,35]) to derive approximations in the form of one or a few ordinary differential equations. For organisms which propagate by binary fission this is done in Ref. [2]. The population growth rate appears to be almost proportional to the individual growth rate. For reproducing species with several live stages (egg, embryo, juvenile, adult) often the birth rate is used as the population growth rate in unstructured model described by an ordinary differential equation. As the body size of a species we use the notion of the ultimate body size of the organisms which make up the population. Food intake rate is proportional to the area of the surface of the organism, while maintenance rate is proportional to the volume of the organism. During growth the ratio between the area and volume changes with volume and as a result there is an ultimate body size where energy derived from food just equals the maintenance costs. For constant food availability the size as a function of age is the so-called von Bertalanffy growth curve.

In Ref. [1], p. 217, body size scaling relationships are derived to compare individual parameters (some of them are shown in Table 1) across species. These relationships have been tested intensively for data on: birds, mammals, reptiles and amphibians, fishes, crustaceans, molluscs. According to the body size scaling relationships, the maximum growth rate (Ref. [1], p. 224) and the

maximum reproductive rate (Ref. [1], p. 236) decrease with ultimate body size while the life span increases. Thus, generally the maximum population growth rate decreases with body size.

In conclusion: the biological constraint that predators tend to be larger than their prey and that larger species grow slower imply that the maximum growth rate is decreasing with the trophic level. This restricts invasibility in longer food chains. Long food chains can exist only when the dilution rate is low and the concentration of the substrate in the reservoir is large.

Comparison of the bifurcation diagrams Figs. 2 and 5 indicate that the term 'organizing centre' used in Ref. [10] for the codimension 2 point, denoted by $M_1$, is appropriate. The global picture around this point seems for food chains of different length qualitatively the same. The invasibility condition for the three types of boundary attractors (point attractor, limit cycle and strange attractor) is that the Lyapunov exponent associated with the invader is positive, that is 'average' growth rate of the invader has to be greater than its depletion rate.

## Acknowledgements

The authors like to thank Hugo van den Berg for valuable discussions. The research of the second author was supported by the Netherlands Organization for Scientific Research (NWO).

## References

[1] S.A.L.M. Kooijman, Dynamic Energy Budgets in Biological Systems: Theory and Applications in Ecotoxicology, Cambridge University, Cambridge, 1993.
[2] B.W. Kooi, S.A.L.M. Kooijman, Existence and stability of microbial prey–predator systems, J. Theor. Biol. 170 (1994) 75.
[3] A. Cunningham, R.M. Nisbet, Transients and oscillations in continuous culture, in: M.J. Bazin (Ed.), Mathematical Methods in Microbiology, 1983, p. 77.
[4] R.M. Nisbet, A. Cunningham, W.S.C. Gurney, Endogenous metabolism and the stability of microbial prey–predator systems, Biotechnol. Bioeng. 25 (1983) 301.
[5] M. Kot, G.S. Sayler, T.W. Schultz, Complex dynamics in a model microbial system, Bull. Math. Biol. 54 (1992) 619.
[6] S. Pavlou, I. Kevrekidis, Microbial predation in a periodically operated chemostat: A global study of the interaction between natural and externally imposed frequencies, Math. Biosci. 108 (1992) 1.
[7] A. Gragnani, S. Rinaldi, A universal bifurcation diagram for seasonally perturbed predator–prey models, Bull. Math. Biology 57 (1995) 701.
[8] M.L. Rosenzweig, R.H. MacArthur, Graphical representation and stability conditions of predator–prey interactions, Am. Natural. 97 (1963) 209.
[9] M.L. Rosenzweig, Exploitation in three trophic levels, Am. Natural. 107 (1973) 275.
[10] K. McCann, P. Yodzis, Bifurcation structure of a tree-species food chain model, Theor. Popul. Biol. 48 (1995) 93.

[11] A. Hastings, T. Powell, Chaos in a three-species food chain, Ecology 72 (1991) 896.
[12] A. Klebanoff, A. Hastings, Chaos in one-predator, two-prey models: general results from bifurcation theory, Math. Biosci. 122 (1994) 221.
[13] A. Klebanoff, A. Hastings, Chaos in three-species food chain, J. Math. Biol. 32 (1994) 427.
[14] Y.A. Kuznetsov, S. Rinaldi, Remarks on food chain dynamics, Math. Biosci. 124 (1996) 1.
[15] P. Yodzis, Introduction to Theoretical Ecology, Harper and Row, New York, 1989.
[16] W.M. Post, S.L. Pimm, Community assembly and food web stability, Math. Biosci. 64 (1983) 169.
[17] E. Doedel, J. Kernévez, Auto: Software for continuation problems in ordinary differential equations with applications, Technical report, California Institute of Technology, Applied Mathematics, 1986.
[18] E.J. Doedel, A.R. Champneys, T.F. Fairgrieve, Y.A. Kuznetsov, B. Sandstede, X. Wang, Auto 97: Continuation and bifurcation software for ordinary differential equations, Technical report, Concordia University, Montreal, Canada, 1997.
[19] A.I. Khibnik, Y.A. Kuznetsov, V.V. Levitin, E.V. Nikolaev, Continuation techniques and interactive software for bifurcation analysis of ODEs and iterated maps, Physica D 62 (1993) 360.
[20] Y.A. Kuznetsov, V.V. Levitin, CONTENT, Centrum voor Wiskunde en Informatica (CWI), 1st ed., Kruislaan 413, 1098 SJ Amsterdam, The Netherlands, 1997.
[21] Y.A. Kuznetsov, Elements of Applied Bifurcation Theory, Applied Mathematical Sciences, vol. 112, Springer, New York, 1995.
[22] B.W. Kooi, M.P. Boer, S.A.L.M. Kooijman, Complex dynamic behaviour of autonomous microbial food chains, J. Math. Biol. 36 (1997) 24.
[23] M.P. Boer, B.W. Kooi, S.A.L.M. Kooijman, Food chain dynamics in the chemostat, Math. Biosci. 150 (1998) 43.
[24] B.W. Kooi, M.P. Boer, S.A.L.M. Kooijman, Consequences of population models on the dynamics of food chains, Math. Biosci. 153 (1998) 99.
[25] H.L. Smith, P. Waltman, The Theory of the Chemostat, Cambridge University, Cambridge, 1994.
[26] V.A.A. Jansen, Effects of dispersal in a tri-tropic metapopulation model, J. Math. Biol. 33 (1995) 195.
[27] J. Hofbauer, K. Sigmund, The Theory of Evolution and Dynamical Systems, Cambridge University, Cambridge, 1988.
[28] J.A. Drake, The mechanism of community assembly and succession, J. Theor. Biol. 147 (1990) 213.
[29] R. Law, R.D. Morton, Permanence and the assembly of ecological communities, Ecology 77 (1996) 762.
[30] R.D. Morton, R. Law, S.L. Pimm, J.A. Drake, On models for assembling ecological communities, Oikos 75 (1996) 493.
[31] O. Diekmann, S.D. Mylius, J.R. ten Donkelaar, Saumon à la Kaitala et Getz, sauce hollandaise (1998).
[32] D.L. DeAngelis, Dynamics of Nutrient Cycling and Food Webs, number 9 in Population and Community Biology series, Chapman and Hall, London, 1992.
[33] G.E. Hutchinson, An Introduction to Population Ecology, Yale University, New Haven, CT, 1978.
[34] J.A.J. Metz, O. Diekmann, The dynamics of physiologically structured populations, Lecture Notes in Biomathematics, vol. 68, Springer, Berlin, 1986.
[35] A.M. Roos de, A gentle introduction to physiologically structured population models, in: S. Tuljapurkar, H. Caswell (Eds.), Structured-Population Models in Marine, Terrestrial, and Freshwater systems, Chapman and Hall, London, 1997, p. 119.